Electronic Research Archive

https://www.aimspress.com/journal/era

ERA, 33(10): 6538–6557.
DOI: 10.3934/era.2025289
Received: 06 August 2025
Revised: 06 October 2025
Accepted: 21 October 2025
Published: 31 October 2025

Research article

Robust data-driven load frequency control of interconnected power systems with Markovian jump parameters

Guobao Liu, Aobo Zhang, Xiaoming Yan*, Shicheng Huo and Huai Liu

College of Electrical and Automation Engineering, Nanjing Normal University, Nanjing 210046, China

* **Correspondence:** Email: xmyan@njnu.edu.cn.

Abstract: This paper focuses on the robust data-driven load frequency control (LFC) of an interconnected power system involving Markovian jump parameters from damaged data by unknown noise. Firstly, due to the changes in system structure, the LFC model for an interconnected power system involving Markovian jump parameters is described. The vehicle-to-grid technique is also applied to regulate the power system frequency by employing the electric vehicles as a new frequency regulation loop in this model. Secondly, a data-driven control method is used to stabilize the Markovian jump power system (MJPS). Drawing on the damaged data corrupted by unknown noise, two robust stability conditions for the MJPS are formulated, corresponding to the energy-bound approach and the instantaneous-bound approach, respectively. Then, the control gains of the system are obtained by the data-based linear matrix inequalities (LMIs). Finally, the effectiveness of the proposed methods is verified by applying them to a two-area interconnected power system with the participation of electric vehicles.

Keywords: data-driven control; LFC; unknown noise; MJPS; data-based LMIs

1. Introduction

With the development of the economy and the increasing demand for electricity, the challenges facing power systems become increasingly complex, especially in the context of the gradual increase in the proportion of renewable energy sources. How to effectively regulate the system frequency to adapt to the dynamic load changes and power fluctuations has become an urgent problem for power engineers. Among that, load frequency control (LFC) plays a crucial role in ensuring the robust stability [1, 2] of power systems. For example, integral [3], proportional-integral [4], proportional-integral-derivative and other control techniques were studied which give the basic analysis of the LFC of the power system. Sliding mode controller [5] and predictive control explore

the basic conventional concepts of LFC. [6, 7] investigated controller design methodologies under denial-of-service attacks.

Electric vehicles (EVs), as common charging and discharging devices in electric power systems, can be used both as electrical equipment and as mobile power sources connected to the grid. The EV is commonly regarded as a disturbance in the power system, which presents significant challenges to the robust stability of the power system. With the advancement of vehicle-to-grid (V2G) technology, more and more researchers have started to study the participation of EVs in the system frequency regulation (FM). The EVs can be used for primary FM by droop control to simulate the operation of a turbine governor. EVs are used as a power source to support the fast response of the power plant to LFC requirements for secondary FM [8]. At the same time, the response frequency speed of EVs is more rapid compared with the traditional FM units.

In recent years, data-driven methods have been applied to control. Data-driven control (DDC) relies more on the data collected during the operation of the system rather than a strict mathematical model. It is able to adapt to rapidly changing environments and conditions and also provides instant feedback and adjustment of the system state through continuous monitoring and analysis of data. Therefore, it has received wide attention. Specifically, some DDC methods based on reinforcement learning were proposed in [9, 10]. Proportional-integral-derivative control was mentioned in [11, 12]. However, the control methods mentioned above are data intensive, and the computational dimensions of the matrices will increase fast when the system dimension is increasing. Alternatively, the fundamental theorem proposed by Willems provides another way to design control protocols for unknown or uncertain systems by pre-collecting inputs and states data [13]. This DDC approach has received much attention due to its reduced computational complexity compared to reinforcement learning control methods. A number of DDC methods have been derived from Willems et al., including robust control [14, 15], model predictive control [16, 17], and event-triggered control [18].

Meanwhile, when considering the problem of DDC, process noise is usually assumed to be measurable [9]. The literature mentioned above did not consider the effects of damaged data by unknown noise, but this is not common in practice. These limitations motivate us to further investigate DDC with unknown noise. [19] presented a new approach to obtain feedback controllers for unknown dynamical systems directly from noisy input/state data. Non-conservative design methods for quadratic stabilization, H_2 and H_∞ control with data-based linear matrix inequalities (LMIs) were derived. However, the parameters in [19] are constant, and it does not take into account the parameter jumps. In practical applications, various faults and trips often occur in the subsystems of a multi-area interconnected power system, affecting the normal operation of the power system. Therefore, the dynamic model of the power system may experience some dynamic jumps, and these unexpected jumps can be modelled stochastically by Markovian processes [20]. So far, great efforts have been made in Markovian jump power system (MJPSs) on various issues such as stability and stabilization analyses [21]. In addition, control problems related to MJPSs have received more and more attention and in-depth research, such as H_∞ control [22], stochastic control [23], model predictive control [24], etc. Moreover, in recent years, research focus has shifted towards integrating MJPSs with DDC [25]. However, none of these methods take into account the presence of unknown noise. To our knowledge, the problem of DDC in MJPSs from damaged data remains largely unexplored. The coexistence of random parameter fluctuations and unknown noise within the system introduces dual uncertainties of both structural and stochastic nature. This inherent complexity renders traditional analytical methods,

which rely upon precise modeling assumptions, largely inapplicable. Thus, constructing a stochastic stability condition by LMIs based on damaged data is challenging, which motivates the present study.

In this paper, our main contribution is the application of data-driven LFC to the MJPS from damaged data by unknown noise. Drawing on the collected state data, this study gives two robust stability criteria, which are presented as LMIs. These criteria apply to noise-affected systems and correspond to two distinct approaches: the energy-bound approach and the instantaneous-bound approach. Using the matrix S-lemma, two data-based LMI conditions are given to ensure that the robust stability criteria hold. The data-driven controllers are designed and solved for feasible state feedback gains. By continuously monitoring and analyzing the data, immediate feedback and adjustment of the MJPS state are achieved. In addition, the V2G technique is used to improve the FM of the power system by employing the EVs as a new FM loop in the secondary FM process of the power system. Finally, the effectiveness of the proposed method is verified by applying it to the MJPS.

Notations: $\mathbb{R}^{m\times n}$ means the set of all $m \times n$ real matrices. The transpose of the matrix and inverse of the matrix are represented by the superscripts T and -1. The occurrence probability of the event N is presented by $Pr(N)$. The appropriate identity matrix is presented by I. The w largest 2-norm is represented by $\sup \|w\|^2$.

2. Problem formulation

2.1. Power system model with EVs

The essence of V2G technology is the bi-directional exchange of information and power between EVs and the power grid through modern control systems. It relies on EVs charging and discharging control devices and communication networks after EVs are connected to the power grid.

Based on the above technology, there are two main control methods used in the current research on EVs participation in grid FM, namely, centralized control and decentralized control. In view of their advantages and disadvantages, we use the virtual power plant as a centralized agent for the centralized control method of EVs.

The dynamic model of an EV's battery system is usually described by the following first-order transfer function:

$$G_{EV}(s) = \frac{K_{EV}}{1 + sT_{EV}}.$$

The simplified model of the multi-area power system is shown in Figure 1, which has the following dynamic equations [26]:

$$
\begin{cases}
\Delta\dot{f}_i(t) = -\dfrac{D_i}{M_i}\Delta f_i(t) + \dfrac{1}{M_i}(\Delta P_{mi}(t) + \Delta P_{EVi}(t) \\
\qquad\qquad - \Delta P_{tie-i}(t)) \\
\Delta\dot{P}_{mi}(t) = \dfrac{1}{T_{chi}}(\Delta P_{vi}(t) - \Delta P_{mi}(t)) \\
\Delta\dot{P}_{vi}(t) = \dfrac{1}{T_{gi}}(\alpha_0 u_i(t) - \Delta P_{vi}(t) - \dfrac{1}{R_i}\Delta f_i(t)) \\
\Delta\dot{P}_{EVi}(t) = -\dfrac{1}{T_{EVi}}P_{EVi}(t) + \dfrac{\alpha_i K_{EVi}}{T_{EVi}}u_i(t) \\
ACE_i(t) = \beta_i\Delta f_i(t) + \Delta P_{tie-i}(t) \\
\Delta\dot{P}_{tie-i}(t) = 2\pi \sum\limits_{j=1,i\neq 1}^{N} T_{ij}\Delta f_i(t).
\end{cases}
$$

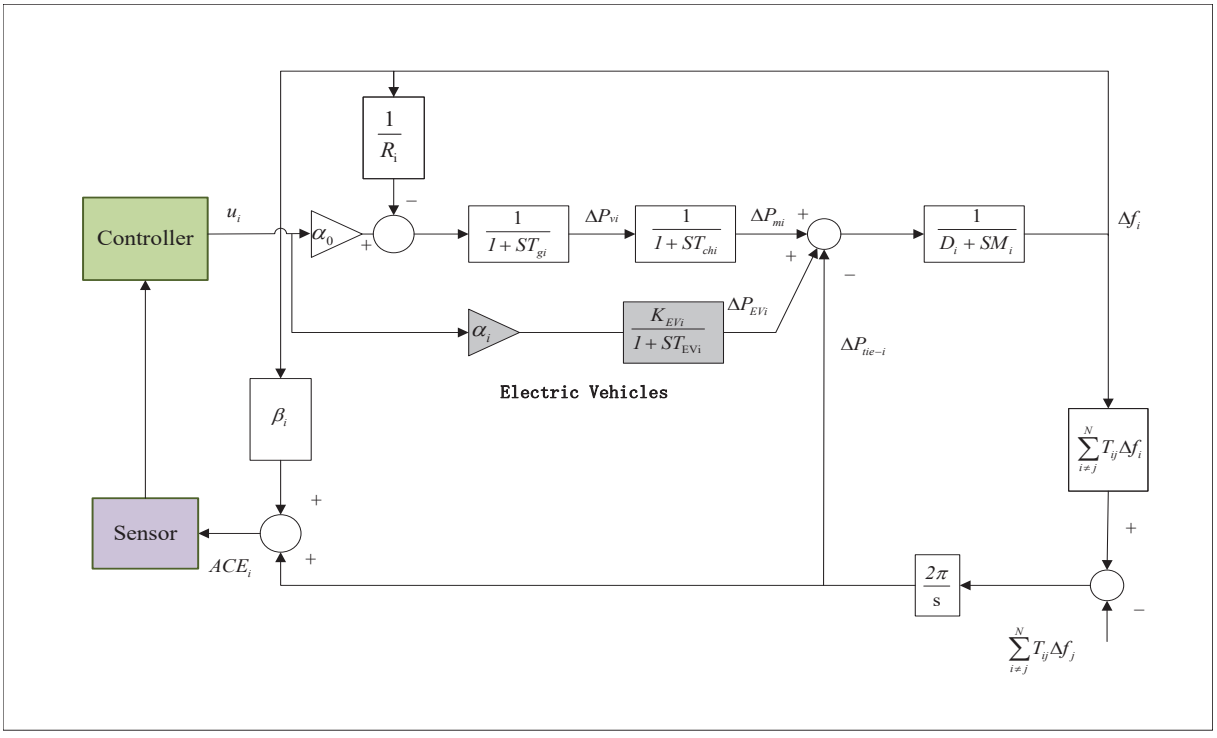

Figure 1. LFC model with EVs participation.

Table 1 reflects the actual meanings expressed by the parameters.

Table 1. Parameters of power systems.

Notation	Name
$\Delta f(t)$	Frequency deviation
$\Delta P_m(t)$	Generator mechanical input deviation
$\Delta P_v(t)$	Valve position deviation
$\Delta P_{EV}(t)$	Fluctuations in EV power output
β	Frequency bias factor
$ACE(t)$	Regional control error
M	Generator moment of inertia
D	Generator damping factor
T_g	Time constant of the regulator
T_{ch}	Time constant of the turbine
T_{EV}	Time Constants for Electric Vehicles
R	Revolutions per minute drop
T_{ij}	Liaison line factor
K_{EV}	The gain of the EV
α_i	Participation factor for region i
N	Representing N regions

Next, the state equation of the power system can be extracted from the LFC model in Figure 1. Here, we let $x(t)$ be the system state and $u(t)$ be the control input, and we distinguish different areas of the power system in the model by judging i and j.

$$\dot{x}(t) = Ax(t) + Bu(t), \tag{2.1}$$

where

$$x(t) = \begin{bmatrix} x_i(t) \\ x_j(t) \end{bmatrix}, \quad u(t) = \begin{bmatrix} u_i(t) \\ u_j(t) \end{bmatrix}.$$

$$x_i(t) = \begin{bmatrix} \Delta f_i(t) & \Delta P_{mi}(t) & \Delta P_{vi}(t) & \Delta P_{EVi}(t) & \int ACE_i(t)dt & \Delta P_{tie-i}(t) \end{bmatrix}^{\top},$$

$$A = \begin{bmatrix} A_{ii} & A_{ij} \\ A_{ji} & A_{jj} \end{bmatrix},$$

$$A_{ii} = \begin{bmatrix} -\frac{D_i}{M_i} & \frac{1}{M_i} & 0 & \frac{1}{M_i} & 0 & -\frac{1}{M_i} \\ 0 & -\frac{1}{T_{chi}} & \frac{1}{T_{chi}} & 0 & 0 & 0 \\ -\frac{1}{T_{gi}R_i} & 0 & -\frac{1}{T_{gi}} & 0 & 0 & 0 \\ 0 & 0 & 0 & -\frac{1}{T_{EVi}} & 0 & 0 \\ \beta_i & 0 & 0 & 0 & 0 & 1 \\ 2\pi \sum_{j=1, j\neq i}^{n} T_{ij} & 0 & 0 & 0 & 0 & 0 \end{bmatrix},$$

$$A_{ij} = A_{ji} = \begin{bmatrix} 0 & 0 & 0 & 0 & 0 & 0 \\ 0 & 0 & 0 & 0 & 0 & 0 \\ 0 & 0 & 0 & 0 & 0 & 0 \\ 0 & 0 & 0 & 0 & 0 & 0 \\ 0 & 0 & 0 & 0 & 0 & 0 \\ -2\pi T_{ij} & 0 & 0 & 0 & 0 & 0 \end{bmatrix},$$

$$B = \begin{bmatrix} B_i \\ B_j \end{bmatrix},$$

$$B_i = \begin{bmatrix} 0 & 0 & \frac{\alpha_0}{T_{gi}} & \frac{K_{EVi}\alpha_i}{T_{EVi}} & 0 & 0 \end{bmatrix}^\top.$$

Inspired by [27], the power system is described as the following discrete-time MJPS:

$$x(k+1) = \bar{\mathcal{A}}(r(k))x(k) + \bar{\mathcal{B}}(r(k))u(k), \quad k = 0, 1, 2, 3 \ldots. \tag{2.2}$$

Here, $\bar{\mathcal{A}}$, $\bar{\mathcal{B}}$ indicate the true but unknown system matrices. The stochastic variable $r(k)$ stands for the Markovian chain and its transition probability matrix $\Gamma = \{\Gamma_{pq}\}_{M\times M}$ is expressed as

$$Pr\{r(k+1) = q | r(k) = p\} = \Gamma_{pq}, \quad 0 \le \Gamma_{pq} \le 1,$$

$$p, q \in \mathcal{M} = \{1, 2, \ldots, M\}, \quad \sum_{q=1}^{M} \Gamma_{pq} = 1.$$

For the presentation convenience, take $r(k) = p$, $\bar{\mathcal{A}}(r(k)) = \bar{\mathcal{A}}_p$, $\bar{\mathcal{B}}(r(k)) = \bar{\mathcal{B}}_p$.

Remark 1: In practice, rapid changes in power demand can affect the operational state of the system. When the load exceeds expectations, it may be necessary to start backup generators or perform load shifting, which triggers a jump in the system state and a change in the system's parameters. In the meantime, various faults and trips often occur in the sub-systems of a multi-area interconnected power system. Some jumps in the parameters of the power system may occur, and these unexpected jumps can be modeled by Markovian processes. To validate the feasibility of our proposed methodology, we selected scenarios where system dynamics exhibit statistical regularity and can be learned from historical data. Consequently, we set the Markov transition probabilities as known.

The data of the system is collected on a time interval, and the collected data is stored in the form of the following matrices:

$$\begin{aligned} \chi_p &:= \begin{bmatrix} x_p(0) & x_p(1) & \ldots & x_p(K-1) \end{bmatrix}, \\ \chi_p^+ &:= \begin{bmatrix} x_p(1) & x_p(2) & \ldots & x_p(K) \end{bmatrix}, \\ \bar{\Omega}_p &:= \begin{bmatrix} w_p(0) & w_p(1) & \ldots & w_p(K-1) \end{bmatrix}, \\ U_p &:= \begin{bmatrix} u_p(0) & u_p(1) & \ldots & u_p(K-1) \end{bmatrix}. \end{aligned}$$

K represents the number of samples collected, and k represents the kth collection moment.

We clearly have

$$\chi_p^+ = \bar{\mathcal{A}}_p\chi_p + \bar{\mathcal{B}}_p U_p + \bar{\Omega}_p. \tag{2.3}$$

For the kth moment

$$x_p(k+1) = \bar{\mathcal{A}}_p x_p(k) + \bar{\mathcal{B}}_p u_p(k) + w_p(k). \tag{2.4}$$

Follow-up articles use w_p for $w_p(k)$. The matrix $\bar{\Omega}_p$ and w_p are unknown, and $\{\bar{\mathcal{A}}_p\}_{p\in\mathcal{M}}$, $\{\bar{\mathcal{B}}_p\}_{p\in\mathcal{M}}$ are the system matrices. Bring $U_p = \mathcal{K}_p\chi_p$ and $u_p = \mathcal{K}_p x_p(k)$ into the above equation of state to obtain the closed-loop system

$$\begin{aligned} \chi_p^+ &= (\bar{\mathcal{A}}_p + \bar{\mathcal{B}}_p\mathcal{K}_p)\chi_p + \bar{\Omega}_p, \\ x_p(k+1) &= (\bar{\mathcal{A}}_p + \bar{\mathcal{B}}_p\mathcal{K}_p)x_p(k) + w_p(k). \end{aligned} \tag{2.5}$$

Remark 2: A similar model for discrete-time systems was introduced in [19]. They proposed a new method to obtain feedback controllers of an unknown dynamical system directly from damaged data. Based on the article, we apply the method to an interconnected power system with Markovian jump parameters. Since the noise is unknown, the controller will be designed from the state and input data that can be collected.

2.2. Assumption on the Noisy

Assumption 1 (Noisy model): For each $p \in \mathcal{M}$, there exist energy-bound $\bar{\Omega}_i \in \mathcal{W}_p$ or an instantaneous-bound $w_p(k) \in W_p$, where

$$\mathcal{W}_p := \left\{ \bar{\Omega}_p \in \mathbb{R}^{n\times K} \middle| \begin{bmatrix} I \\ {\Omega_p}^\top \end{bmatrix}^\top \Psi^p \begin{bmatrix} I \\ {\Omega_p}^\top \end{bmatrix} \geq 0 \right\}, \tag{2.6}$$

$$W_p := \left\{ w_p \in \mathbb{R}^n \middle| \begin{bmatrix} I \\ {w_p}^\top \end{bmatrix}^\top \Psi^p \begin{bmatrix} I \\ {w_p}^\top \end{bmatrix} \geq 0 \right\}. \tag{2.7}$$

For some known matrices $\Psi^p_{1,1} = {\Psi^p_{1,1}}^\top$, $\Psi^p_{1,2}$, $\Psi^p_{2,2} = {\Psi^p_{2,2}}^\top < 0$,
where

$$\Psi^p = \begin{bmatrix} \Psi^p_{1,1} & \Psi^p_{1,2} \\ {\Psi^p_{1,2}}^\top & \Psi^p_{2,2} \end{bmatrix}.$$

Remark 3: The specific application of the energy-bounded model in Assumption 1 is as follows: when designing LFC controllers, random load variations can be modelled as energy-bounded disturbances. The controller is designed to maintain frequency deviation and regional control error within acceptable limits even under worst-case load fluctuations. The specific application of the instantaneous-bounded model in Assumption 1 is as follows: In power system state estimation, measurement errors are assumed to have known upper and lower bounds. The output is not an optimal estimate but a state interval, guaranteeing that the true state lies within this range. During current surges caused by lightning strikes, the amplitude can theoretically reach extremely high levels, far exceeding the boundaries of conventional load fluctuations or measurement errors. The current model becomes inapplicable in such scenarios. However, our primary objective focuses on constructing a controllable and reproducible environment to validate the methodology. Therefore, this phenomenon is not considered in this paper. In this case, Assumption 1, for general norm-bounded noise $\sup \|w_p\|^2 \leq \overline{w}_p$, we divide the noise constraint into two cases. The energy-bound approach holds with $\Psi^p_{1,1} = K\overline{w}_p I$, $\Psi^p_{1,2} = 0$, $\Psi^p_{2,2} = -I$. The instantaneous-bound approach holds with $\Psi^p_{1,1} = \overline{w}_p I$,

$\Psi^p_{1,2} = 0$, $\Psi^p_{2,2} = -I$. Descriptions of noisy data can also be found in [19]. We further extend this to the robust DDC of the MJPS involving EVs.

Define, for the energy-bound approach, with each $p \in M$, the compatibility set

$$C_p := \{(\mathcal{A}_p, \mathcal{B}_p) \mid \exists \Omega_p \in \mathcal{W}_p : \chi_p^+ = \mathcal{A}_p\chi_p + \mathcal{B}_p U_p + \Omega_p\} = \{(\mathcal{A}_p, \mathcal{B}_p) \mid (2.3) \text{ holds}\}. \tag{2.8}$$

Define, for the instantaneous-bound approach, with each $p \in M$, the compatibility set

$$\begin{aligned} C_{pk} := \{(\mathcal{A}_p, \mathcal{B}_p) \mid \exists w_p \in \mathcal{W}_p : x_p(k+1) = \mathcal{A}_p x_p(k) \\ + \mathcal{B}_p u_p(k) + w_p(k)\} = \{(\mathcal{A}_p, \mathcal{B}_p) \mid (2.4)\text{holds}\}. \end{aligned} \tag{2.9}$$

Subsequent studies need to use the following lemma.

Lemma 1 (Matrix S-lemma [19]): Let G, N be symmetric. Consider the following:

(a) $\exists \alpha \geq 0, \beta > 0$, such that $G - \alpha N \geqslant \begin{bmatrix} \beta I & 0 \\ 0 & 0 \end{bmatrix}$.

(b) $\begin{bmatrix} I \\ Z \end{bmatrix}^\top G \begin{bmatrix} I \\ Z \end{bmatrix} > 0, \forall Z \in \mathbb{R}^{n\times k}$ such that $\begin{bmatrix} I \\ Z \end{bmatrix}^\top N \begin{bmatrix} I \\ Z \end{bmatrix} \geq 0$.

Then (a) $\Rightarrow$ (b).

Lemma 2 (Matrix S-lemma [28]): Let G, N_k be symmetric, where the matrix N_k depends on the index k. Consider the following:

(a) $\exists \alpha \geq 0, \tau_k > 0$, such that $G - \sum_{k=0}^{K-1} \tau_k N_k \geqslant \begin{bmatrix} \beta I & 0 \\ 0 & 0 \end{bmatrix}$.

(b) $\begin{bmatrix} I \\ Z \end{bmatrix}^\top G \begin{bmatrix} I \\ Z \end{bmatrix} > 0, \forall Z \in \mathbb{R}^{n\times k}$ such that $\begin{bmatrix} I \\ Z \end{bmatrix}^\top N_k \begin{bmatrix} I \\ Z \end{bmatrix} \geq 0$.

Then (a) $\Rightarrow$ (b).

3. Data-driven stabilization

In the set C_p, we have

$$\chi_p^+ = \mathcal{A}_p\chi_p + \mathcal{B}_p U_p + \Omega_p. \tag{3.1}$$

Substitute (3.1) into Assumption 1, one has

$$\begin{bmatrix} I \\ \mathcal{A}_p^\top \\ \mathcal{B}_p^\top \\ 0 \end{bmatrix}^\top \begin{bmatrix} I & \chi_p^+ \\ 0 & -\chi_p \\ 0 & -U_p \\ 0 & 0 \end{bmatrix} \Psi^p \begin{bmatrix} I & \chi_p^+ \\ 0 & -\chi_p \\ 0 & -U_p \\ 0 & 0 \end{bmatrix}^\top \begin{bmatrix} I \\ \mathcal{A}_p^\top \\ \mathcal{B}_p^\top \\ 0 \end{bmatrix} \geq 0, \tag{3.2}$$

Assume that (U_p, χ_p) satisfies (3.2) for some Ω_p satisfying Assumption 1. The data (U_p, χ_p) are called informative for robust stabilization if there exists a feedback gain $\mathcal{K}_p$ and a matrix $P_p > 0$ such that [29]

$$P_p - (\mathcal{A}_p + \mathcal{B}_p\mathcal{K}_p)(\sum_{p=1}^{M} \Gamma_{pq} P_q)(\mathcal{A}_p + \mathcal{B}_p\mathcal{K}_p)^\top > 0. \tag{3.3}$$

Next, the data-driven controller design is presented. For brevity, we define

$$\mathcal{A}_p^{\text{cl}} := \mathcal{A}_p + \mathcal{B}_p\mathcal{K}_p,$$

$$P_p^{\mathrm{cl}} = \sum_{q=1}^{M} \Gamma_{pq} P_q.$$

For the energy-bound approach, we have Theorem 1.

Theorem 1: Suppose the Assumption 1 holds. For all $(\mathcal{A}_p, \mathcal{B}_p) \in C_p$, the MJPS (2.3) is stochastically stable, if there exist matrices $D_p > 0$, D_p^{cl}, L_p, and the scalars $\alpha \geq 0$, $\beta > 0$, and satisfying the following LMI:

$$G_p - \alpha N_p \geq 0, \quad p \in \mathcal{M}, \tag{3.4}$$

where

$$G_p = \begin{bmatrix} D_p^{\mathrm{cl}} - \beta I & 0 & 0 & 0 \\ * & -D_p & -L_p^{\top} & 0 \\ * & * & 0 & L_p \\ * & * & * & D_p \end{bmatrix} > 0, \tag{3.5}$$

$$N_p = \begin{bmatrix} I & \chi_p^{+} \\ 0 & -\chi_p \\ 0 & -U_p \\ 0 & 0 \end{bmatrix} \Psi^p \begin{bmatrix} I & \chi_p^{+} \\ 0 & -\chi_p \\ 0 & -U_p \\ 0 & 0 \end{bmatrix}^{\top} \geq 0. \tag{3.6}$$

Then the control gain matrix $\mathcal{K}_p = L_p D_p^{-1}$ can be acquired.

Proof. It is easy to find that (3.3) is equivalent to

$$\begin{bmatrix} P_p & \mathcal{A}_p^{\mathrm{cl}} P_p^{\mathrm{cl}} \\ * & P_p^{\mathrm{cl}} \end{bmatrix} > 0. \tag{3.7}$$

Let $D_p = P_p^{-1}$, we can obtain that

$$\begin{bmatrix} I \\ \mathcal{A}_p^{\top} \\ \mathcal{B}_p^{\top} \end{bmatrix}^{\top} \begin{bmatrix} D_p^{\mathrm{cl}} & 0 & 0 \\ * & -D_p & -D_p \mathcal{K}_p^{\top} \\ * & * & -\mathcal{K}_p D_p \mathcal{K}_p^{\top} \end{bmatrix} \begin{bmatrix} I \\ \mathcal{A}_p^{\top} \\ \mathcal{B}_p^{\top} \end{bmatrix} > 0. \tag{3.8}$$

Let

$$\mathcal{K}_p = L_p D_p^{-1}, \tag{3.9}$$

then

$$\begin{bmatrix} I \\ \mathcal{A}_p^{\top} \\ \mathcal{B}_p^{\top} \end{bmatrix}^{\top} \begin{bmatrix} D_p^{\mathrm{cl}} & 0 & 0 \\ * & -D_p & -L_p^{\top} \\ * & * & -L_p D_p^{-1} L_p^{\top} \end{bmatrix} \begin{bmatrix} I \\ \mathcal{A}_p^{\top} \\ \mathcal{B}_p^{\top} \end{bmatrix} > 0. \tag{3.10}$$

By applying the Schur complement lemma to the above inequality, we can obtain

$$\begin{bmatrix} D_p^{\mathrm{cl}} & 0 & 0 & 0 \\ * & -D_p & -L_p^{\top} & 0 \\ * & * & 0 & L_p \\ * & * & * & D_p \end{bmatrix} > 0. \tag{3.11}$$

It can be known from Lemma 1 that (3.11) holds if and only if there exist scalars $\alpha \geq 0, \beta > 0$ satisfied

$$\begin{bmatrix} {D_p}^{\mathrm{cl}} & 0 & 0 & 0 \\ * & -D_p & -{L_p}^{\top} & 0 \\ * & * & 0 & L_p \\ * & * & * & D_p \end{bmatrix} - \alpha \begin{bmatrix} I & \chi_p^{+} \\ 0 & -\chi_p \\ 0 & -U_p \\ 0 & 0 \end{bmatrix} \Psi^p \begin{bmatrix} I & \chi_p^{+} \\ 0 & -\chi_p \\ 0 & -U_p \\ 0 & 0 \end{bmatrix}^{\top} \geq 0. \tag{3.12}$$

This means that the feasible control gain $\mathcal{K}_p$ found to stabilize all $(\mathcal{A}_p, \mathcal{B}_p) \in C_p$ using only the data (U_p, χ_p).

This proof is completed.

For the instantaneous-bound approach, we have Theorem 2.

Theorem 2: Suppose the Assumption 1 holds. For all $(\mathcal{A}_p, \mathcal{B}_p) \in C_{pk}$, the MJPS (2.4) is stochastically stable, if there exist matrices $D_p > 0$, ${D_p}^{\mathrm{cl}}$, L_p, and the scalars $\tau_k \geq 0, \beta > 0$, and satisfying the following LMI:

$$G_p - \sum_{k=0}^{K-1} \tau_k N_{p2} \geq 0, \quad p \in \mathcal{M}, \tag{3.13}$$

where

$$G_p = \begin{bmatrix} {D_p}^{\mathrm{cl}} - \beta I & 0 & 0 & 0 \\ * & -D_p & -{L_p}^{\top} & 0 \\ * & * & 0 & L_p \\ * & * & * & D_p \end{bmatrix} > 0, \tag{3.14}$$

$$N_{p2} = \begin{bmatrix} I & x_p(k+1) \\ 0 & -x_p(k) \\ 0 & -u_p(k) \\ 0 & 0 \end{bmatrix} \Psi^p \begin{bmatrix} I & x_p(k+1) \\ 0 & -x_p(k) \\ 0 & -u_p(k) \\ 0 & 0 \end{bmatrix}^{\top} \geq 0. \tag{3.15}$$

The proof process is similar to Theorem 1.

Remark 4: With respect to (3.4), solving (3.13) involves K variables τ_k instead of a single one α. Having as many decision variables as data points is demanding on decision variables.

Remark 5: These two theorems correspond respectively to the energy-bound method and the instantaneous-bound method. The energy-bound method examines the total impact of a signal throughout its entire temporal evolution, primarily analyzing the stability and performance of a system under finite modelling errors or external disturbances. The instantaneous-bound method constrains the instantaneous amplitude of the signal at any given moment within a known range, investigating the potential influence of the signal at each individual point in time.

4. Numerical examples

In this section, a numerical example is employed to illustrate the validity of the control design method for a two-area interconnected MJPS. The required power system parameters are in [26].

In reality, a variety of circumstances will lead to uncertainty about our parameters. Therefore, we cannot determine the state of the parameter matrices A and B. For an interconnected power system with two modes. Consider the transfer parameters and their impacts.

For mode one, $D_1 = 2$; $M_1 = 2$; $R_1 = 1$; $T_{g1} = 0.2$; $T_{ch1} = 0.4$; $T_{EV1} = 1$; $K_{EV1} = 1$; $\beta_1 = 3$; $D_2 = 2$; $M_2 = 2$; $R_2 = 1$; $T_{g2} = 0.2$; $T_{ch2} = 0.5$; $T_{EV2} = 1$; $K_{EV2} = 1$; $\beta_2 = 3$.

For mode two, $D_1 = 2$; $M_1 = 2$; $R_1 = 1$; $T_{g1} = 0.2$; $T_{ch1} = 0.4$; $T_{EV1} = 1$; $K_{EV1} = 1$; $\beta_1 = 3$; $D_2 = 1.5$; $M_2 = 2$; $R_2 = 1$; $T_{g2} = 0.25$; $T_{ch2} = 0.45$; $T_{EV2} = 1$; $K_{EV2} = 1$; $\beta_2 = 2.5$.

In the simulation case, we set the sampling interval to 0.05 s. The above parameters are state parameters in the continuous time, and we need to discretize them. This paper employs the zero-order hold method to discretize the continuous-time system model. This approach assumes that the control input remains constant over the sampling interval, aligning with practical control systems and representing the most commonly used discretization method in engineering practice. However, during the controller gain solution, the parameters of the MJPS are unknown, but the state data are known. Therefore, we have to get the control gain from the collected damaged data. During the data collection phase, the initial states as well as the inputs of the followers are randomly generated.

For the energy-bound approach, by solving the LMI-based damaged data in (3.4), we obtain a set of feasible control gain matrices:

$$\mathcal{K}_{e1} = \begin{bmatrix} K_{e1}^1 & K_{e1}^2 \\ K_{e1}^3 & K_{e1}^4 \end{bmatrix}, \mathcal{K}_{e2} = \begin{bmatrix} K_{e2}^1 & K_{e2}^2 \\ K_{e2}^3 & K_{e2}^4 \end{bmatrix},$$

$$K_{e1}^1 = \begin{bmatrix} -0.054 & 0.009 & -0.815 & -0.080 & -0.223 & 0.411 \end{bmatrix},$$

$$K_{e1}^2 = \begin{bmatrix} -0.743 & -0.302 & 0.491 & 1.515 & -0.094 & 0.369 \end{bmatrix},$$

$$K_{e1}^3 = \begin{bmatrix} -0.531 & -0.146 & 0.279 & 0.732 & 0.031 & -0.072 \end{bmatrix},$$

$$K_{e1}^4 = \begin{bmatrix} -0.121 & 0.002 & -0.691 & -0.050 & -0.335 & 0.230 \end{bmatrix},$$

$$K_{e2}^1 = \begin{bmatrix} -1.637 & -0.418 & 1.052 & 2.057 & 0.073 & -1.300 \end{bmatrix},$$

$$K_{e2}^2 = \begin{bmatrix} 0.163 & 0.049 & -0.406 & -0.196 & 0.177 & -0.899 \end{bmatrix},$$

$$K_{e2}^3 = \begin{bmatrix} -0.050 & -0.019 & 0.652 & 0.099 & -0.100 & 0.564 \end{bmatrix},$$

$$K_{e2}^4 = \begin{bmatrix} -0.244 & -0.055 & 0.064 & 0.186 & -0.310 & 0.626 \end{bmatrix}.$$

For the instantaneous-bound approach, by solving the LMI-based damaged data in (3.12), we obtain a set of feasible control gain matrices:

$$\mathcal{K}_{b1} = \begin{bmatrix} K_{b1}^1 & K_{b1}^2 \\ K_{b1}^3 & K_{b1}^4 \end{bmatrix}, \mathcal{K}_{b2} = \begin{bmatrix} K_{b2}^1 & K_{b2}^2 \\ K_{b2}^3 & K_{b2}^4 \end{bmatrix},$$

$$K_{b1}^1 = \begin{bmatrix} 441.198 & 121.824 & 76.686 & -621.811 & -192.403 & 857.341 \end{bmatrix},$$

$$K_{b1}^2 = \begin{bmatrix} 143.540 & 51.114 & -138.297 & -252.865 & -69.685 & 625.313 \end{bmatrix},$$

$$K_{b1}^3 = \begin{bmatrix} -726.127 & -193.704 & -40.838 & 967.256 & 161.268 & -906.159 \end{bmatrix},$$

$$K_{b1}^4 = \begin{bmatrix} -455.198 & -167.137 & 303.992 & 821.155 & -1.827 & -594.690 \end{bmatrix},$$

$$K_{b2}^1 = \begin{bmatrix} -111.025 & -30.197 & -127.750 & 148.907 & 111.591 & -519.799 \end{bmatrix},$$

$$K_{b2}^2 = \begin{bmatrix} -31.808 & -9.918 & -20.963 & 38.701 & 87.962 & -437.998 \end{bmatrix},$$
$$K_{b2}^3 = \begin{bmatrix} 89.652 & 24.063 & -18.065 & -119.915 & -13.727 & 84.327 \end{bmatrix},$$
$$K_{b2}^4 = \begin{bmatrix} 51.694 & 20.792 & -72.656 & -112.148 & -2.450 & 53.598 \end{bmatrix}.$$

In all numerical simulations, the system's initial state vector x and external input u are both randomly generated from a standard normal distribution. Moreover, our simulation conducted a comparative analysis for noise boundaries of 0.1 and 0.05.

In Figure 2, the switching process of the MJPS is illustrated. For the energy-constrained method, as shown in Figures 3 and 4, after introducing our designed controller, the frequency deviation with a noise boundary of 0.1 approaches zero within 7.5 seconds, while that with a noise boundary of 0.05 approaches zero within 6 seconds. Moreover, as depicted in Figures 5 and 6, the $\Delta P_m(t)$ with a noise boundary of 0.1 converges to zero within 5 seconds; the $\Delta P_m(t)$ with a noise boundary of 0.05 converges to zero within 3 seconds. For the instantaneous constraint strategy, as depicted in Figures 7 and 8, after introducing our designed controller, the frequency deviation with a noise boundary of 0.1 approaches zero within 7.5 seconds, while that with a noise boundary of 0.05 approaches zero within 5 seconds. Furthermore, as depicted in Figures 9 and 10, the $\Delta P_m(t)$ with a noise boundary of 0.1 converges to zero within 4 seconds; the $\Delta P_m(t)$ with a noise boundary of 0.05 converges to zero within 3.5 seconds. In summary, the LFC strategy proposed in this paper is able to make full use of the FM capability of both conventional units and EVs. So the MJPS reaches robust stability, which proves the feasibility of our control method.

Remark 6: The paper aims to address the practical challenge of obtaining precise model parameters in LFC. Its primary objective is to validate the methodology's feasibility. In contrast to model-reliant approaches such as H_∞ control, its data-driven nature enables robust handling of both model inaccuracies and parameter jumps, thereby substantially extending its applicability. Furthermore, compared to existing data-driven strategies that typically require known noise assumptions, our approach overcomes this critical limitation by operating directly on measurement data alone. These characteristics significantly enhance the method's engineering utility.

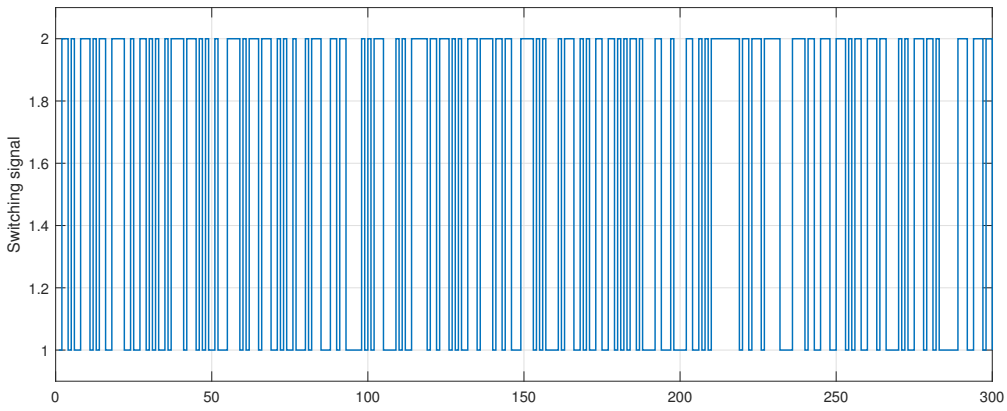

Figure 2. Switching signal.

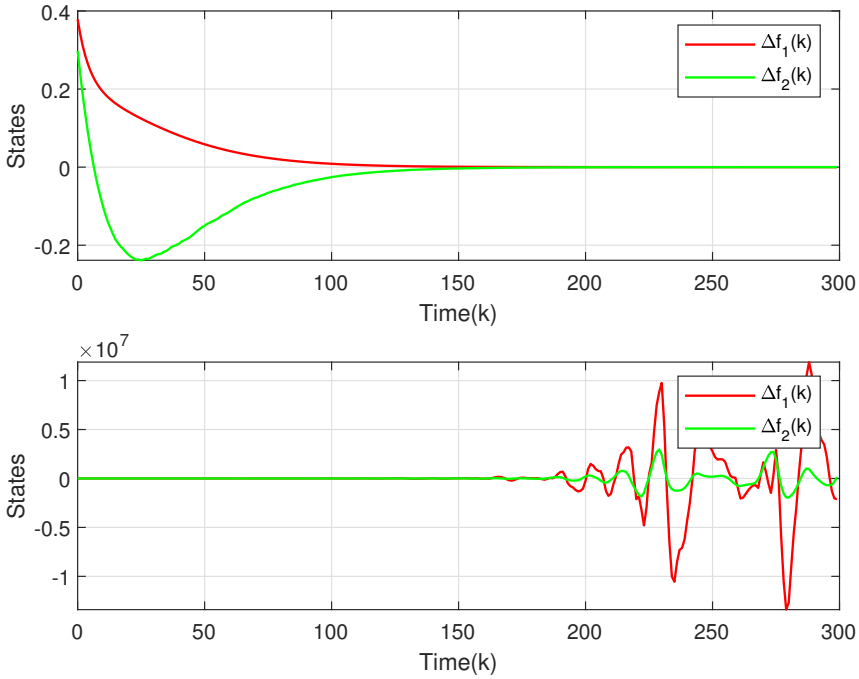

Figure 3. Frequency deviation signal for the energy-bound approach 0.1.

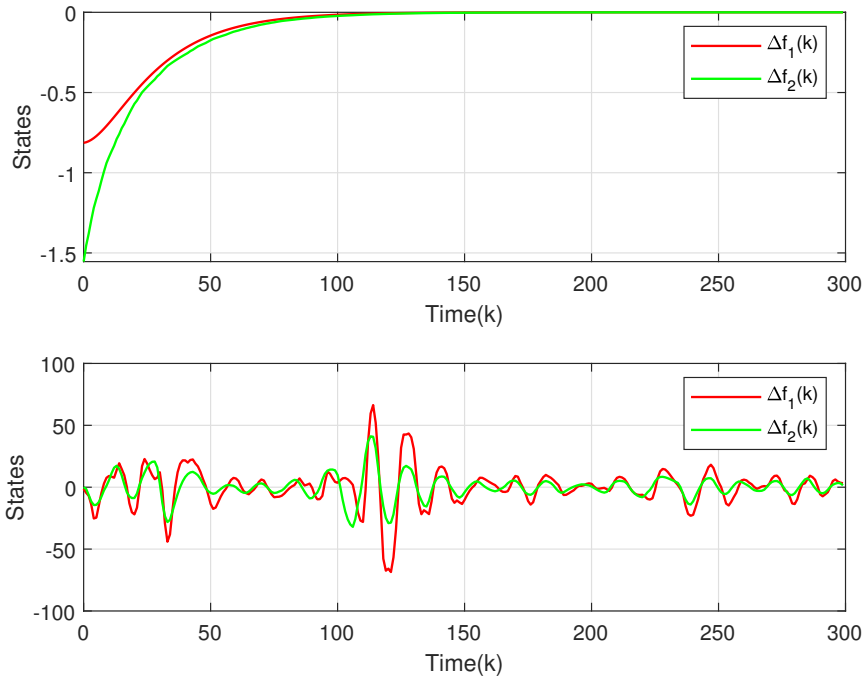

Figure 4. Frequency deviation signal for the energy-bound approach 0.05.

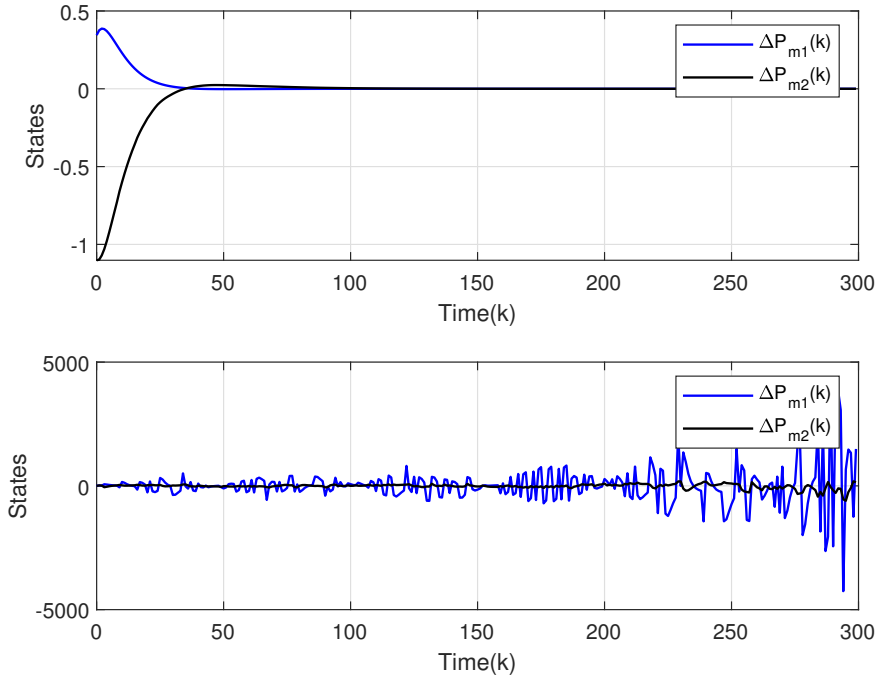

Figure 5. Generator mechanical input deviation signal for the energy-bound approach 0.1.

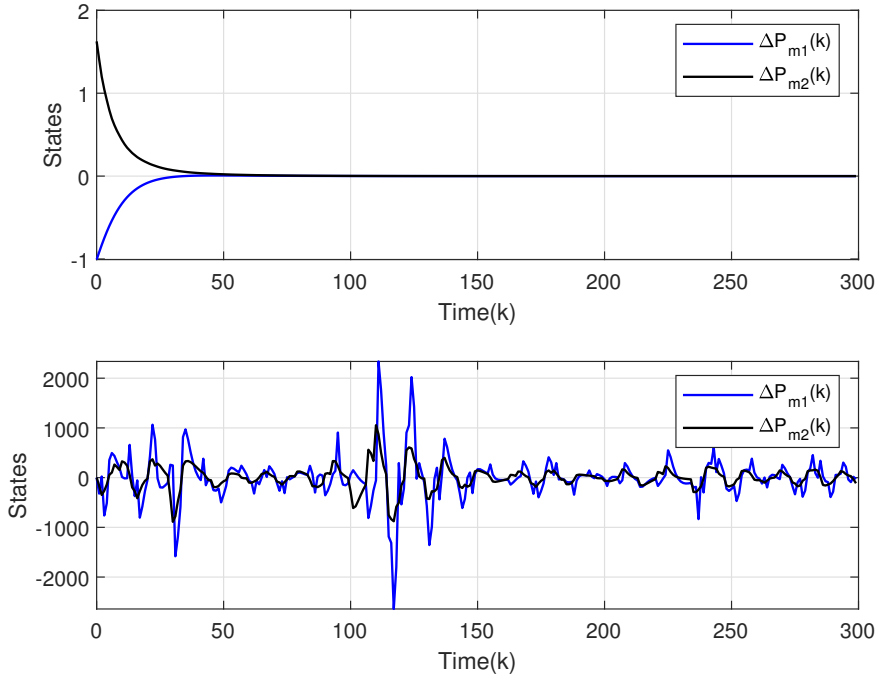

Figure 6. Generator mechanical input deviation signal for the energy-bound approach 0.05.

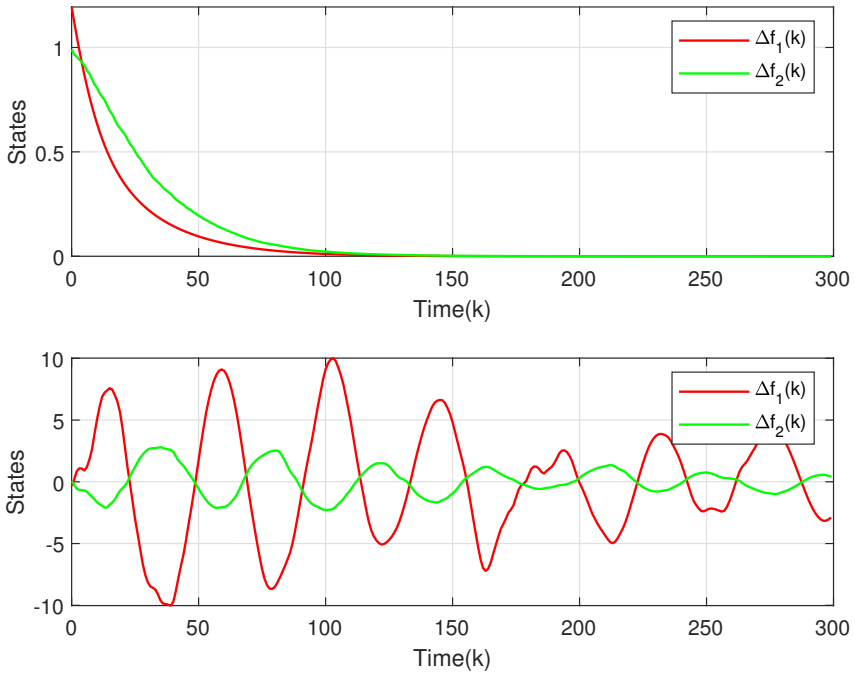

Figure 7. Frequency deviation signal for the instantaneous-bound approach 0.1.

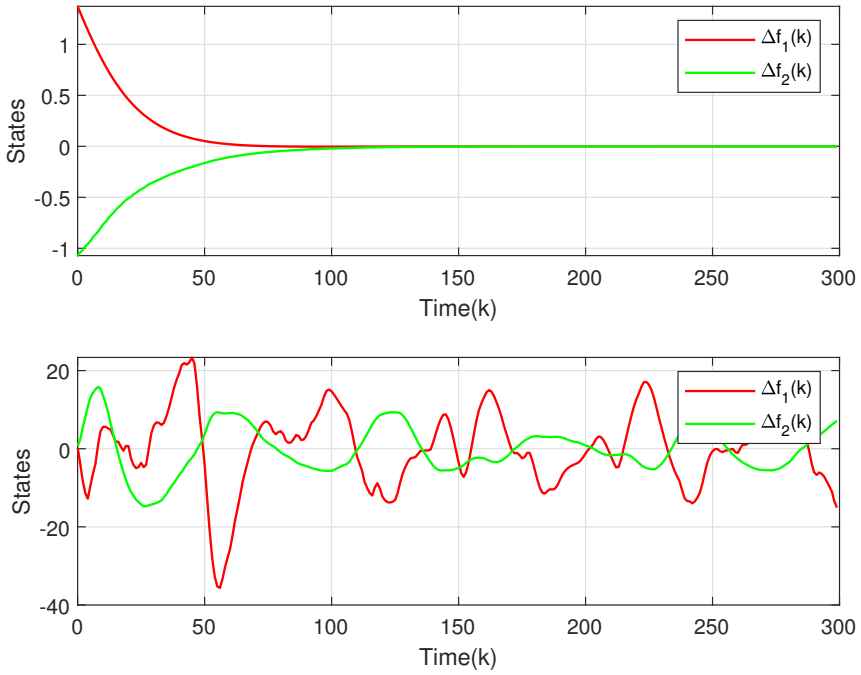

Figure 8. Frequency deviation signal for the instantaneous-bound approach 0.05.

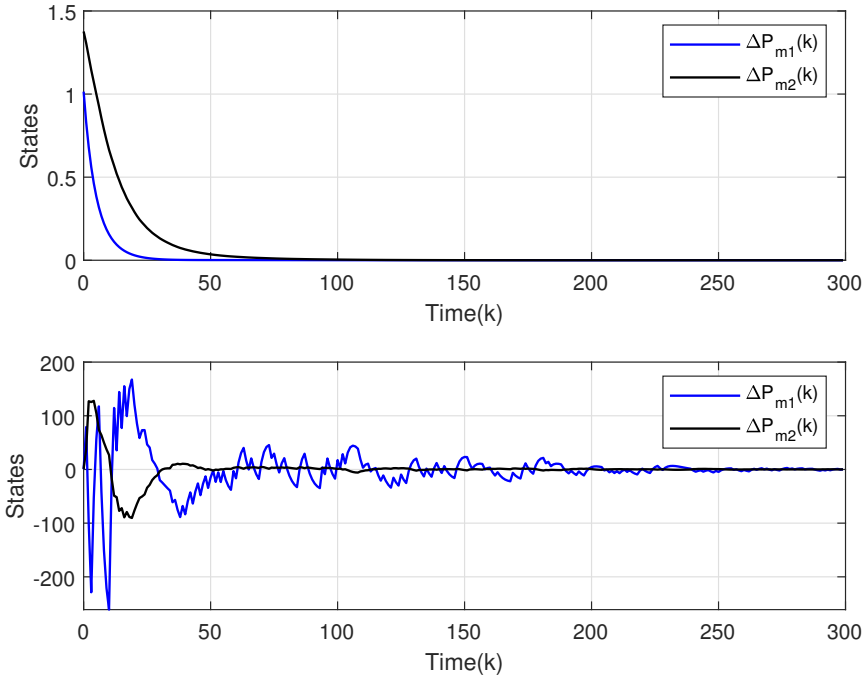

Figure 9. Generator mechanical input deviation signal for the instantaneous-bound approach 0.1.

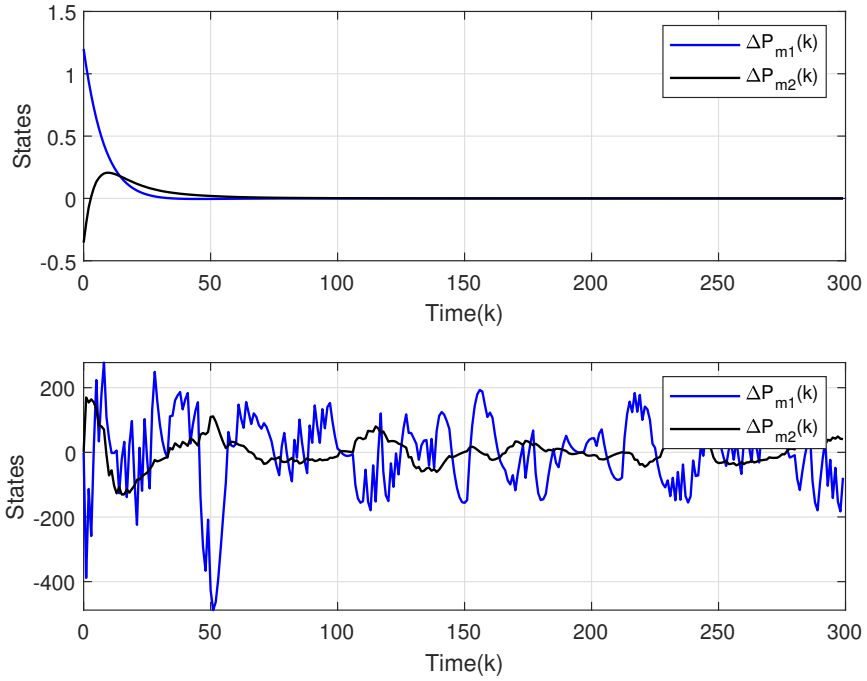

Figure 10. Generator mechanical input deviation signal for the instantaneous-bound approach 0.05.

5. Conclusions

In this paper, a data-driven load frequency controller based on damaged data by unknown noise has been designed for a power system with uncertain Markovian jump parameters. The robust stability condition of the MJPS has been constructed in the form of an LMI based on the damaged data. The control gain matrix has been determined by solving the data-based LMI. And the effectiveness of the strategy proposed in this paper in the MJPS has been verified by applying it to a two-area interconnected power system with the participation of EVs. But for complex systems such as high-dimensional, multi-agent systems, the scale of corresponding LMI problems increases dramatically, leading to prolonged solution times and even numerical instability. Consequently, it is imperative that future approaches integrate the aforementioned DDC methods with event-triggered [30, 31] or distributed control [32].

Use of AI tools declaration

The authors declare they have not used Artificial Intelligence (AI) tools in the creation of this article.

Acknowledgments

This work was supported in part by the National Natural Science Foundation of China under Grants 52507062, 62503234, 62473198 and 62003168; the Natural Science Foundation of Jiangsu Province under Grant BK20230378; the Natural Science Research Project of Jiangsu Higher Education Institutions under Grants 23KJB470022 and 23KJB120006.

Conflict of interest

The authors declare no conflicts of interest.

References

1. G. Zhang, Y. Xing, W. Zhang, J. Li, Prescribed performance control for USV-UAV via a robust bounded compensating technique, *IEEE Trans. Control Network Syst.*, **12** (2025), 2289–2299. https://doi.org/10.1109/TCNS.2025.3566320
2. S. Park, C. Park, J. Kim, Learning-based cooperative mobility control for autonomous drone-delivery, *IEEE Trans. Veh. Technol.*, **73** (2024), 4870–4885. https://doi.org/10.1109/TVT.2023.3330460
3. G. Zhang, Z. Li, J. Li, Y. Shu, X. Zhang, Reinforcement learning-driven autonomous navigation strategy for rotor-assisted vehicles via integral event-triggered mechanism, *Transp. Res. Part D: Transp. Environ.*, **146** (2025), 104841. https://doi.org/10.1016/j.trd.2025.104841
4. B. K. Priya, D. A. Reddy, W. G. Soliman, A. D. Rani, N. Kalahasthi, D. V. R. K. Reddy, Hybrid stepper motor: Model, open-loop test, traditional PI, optimized PI, and optimized gain scheduled PI controllers, *Int. J. Control Autom. Syst.*, **20** (2022), 3915–3922. https://doi.org/10.1007/s12555-021-0371-y

5. W. Qi, G. Zong, H. R. Karimi, Sliding mode control for nonlinear stochastic singular semi-Markov jump systems, *IEEE Trans. Autom. Control*, **65** (2020), 361–368. https://doi.org/10.1109/TAC.2019.2915141
6. X. Cai, K. Shi, Y. Sun, J. Cao, S. Wen, Z. Tian, Intelligent event-triggered control supervised by mini-batch machine learning and data compression mechanism for T-S fuzzy NCSs under DoS attacks, *IEEE Trans. Fuzzy Syst.*, **32** (2024), 804–815. https://doi.org/10.1109/TFUZZ.2023.3308933
7. X. Cai, K. Shi, Y. Sun, J. Cao, S. Wen, C. Qiao, et al., Stability analysis of networked control systems under DoS attacks and security controller design with mini-batch machine learning supervision, *IEEE Trans. Inf. Forensics Secur.*, **19** (2024), 3857–3865. https://doi.org/10.1109/TIFS.2023.3347889
8. T. N. Pham, H. Trinh, L. V. Hien, Load frequency control of power systems With electric vehicles and diverse transmission links using distributed functional observers, *IEEE Trans. Smart Grid*, **7** (2016), 238–252. https://doi.org/10.1109/TSG.2015.2449877
9. P. Yu, S. Tan, J. Guo, Y. Song, Data-driven optimal controller design for sub-satellite deployment of tethered satellite system, *Electron. Res. Arch.*, **32** (2024), 505–522. https://doi.org/10.3934/era.2024025
10. A. Sacco, F. Esposito, G. Marchetto, P. Montuschi, Sustainable task offloading in UAV networks via multi-agent reinforcement learning, *IEEE Trans. Veh. Technol.*, **70** (2021), 5003–5015. https://doi.org/10.1109/TVT.2021.3074304
11. L. H. Keel, S. P. Bhattacharyya, Controller synthesis free of analytical models: Three term controllers, *IEEE Trans. Autom. Control*, **53** (2008), 1353–1369. https://doi.org/10.1109/TAC.2008.925810
12. M. Cui, M. Pan, J. Wang, P. Li, A parameterized level set method for structural topology optimization based on reaction diffusion equation and fuzzy PID control algorithm, *Electron. Res. Arch.*, **30** (2022), 2568–2599. https://doi.org/10.3934/era.2022132
13. J. C. Willems, P. Rapisarda, I. Markovsky, B. L. M. De Moor, A note on persistency of excitation, *Syst. Control Lett.*, **54** (2005), 325–329. https://doi.org/10.1016/j.sysconle.2004.09.003
14. C. De Persis, P. Tesi, Formulas for data-driven control: Stabilization, optimality, and robustness, *IEEE Trans. Autom. Control*, **65** (2020), 909–924. https://doi.org/10.1109/TAC.2019.2959924
15. J. G. Rueda-Escobedo, E. Fridman, J. Schiffer, Data-driven control for linear discrete-time delay systems, *IEEE Trans. Autom. Control*, **67** (2022), 3321–3336. https://doi.org/10.1109/TAC.2021.3096896
16. W. Liu, J. Sun, G. Wang, F. Bullo, J. Chen, Data-driven resilient predictive control under denial-of-service, *IEEE Trans. Autom. Control*, **68** (2023), 4722–4737. https://doi.org/10.1109/TAC.2022.3209399
17. K. Hu, T. Liu, Robust data-driven predictive control for unknown linear time-invariant systems, *Syst. Control Lett.*, **193** (2024), 105914. https://doi.org/10.1016/j.sysconle.2024.105914

18. X. Wang, J. Berberich, J. Sun, G. Wang, F. Allgöwer, J. Chen, Model-based and data-driven control of event- and self-triggered discrete-time linear systems, *IEEE Trans. Cybern.*, **53** (2023), 6066–6079. https://doi.org/10.1109/TCYB.2023.3272216
19. H. J. van Waarde, M. K. Camlibel, M. Mesbahi, From noisy data to feedback controllers: Nonconservative design via a matrix S-lemma, *IEEE Trans. Autom. Control*, **67** (2022), 162–175. https://doi.org/10.1109/TAC.2020.3047577
20. R. Sakthivel, P. Selvaraj, O. M. Kwon, S. G. Choi, R. Sakthivel, Robust memory control design for semi-Markovian jump systems with cyber attacks, *Electron. Res. Arch.*, **31** (2023), 7496–7510. https://doi.org/10.3934/era.2023378
21. M. Shen, J. H. Park, H_∞ filtering of Markov jump linear systems with general transition probabilities and output quantization, *ISA Trans.*, **63** (2016), 204–210. https://doi.org/10.1016/j.isatra.2016.04.007
22. G. Wang, L. Xu, Almost sure stability and stabilization of Markovian jump systems with stochastic switching, *IEEE Trans. Autom. Control*, **67** (2022), 1529–1536. https://doi.org/10.1109/TAC.2021.3069705
23. O. L. V. Costa, E. O. A. Filho, E. K. Boukas, R. P. Marques, Constrained quadratic state feedback control of discrete-time Markovian jump linear systems, *Automatica*, **35** (1999), 617–626. https://doi.org/10.1016/S0005-1098(98)00202-7
24. B. Zhang, Y. Song, Model-predictive control for Markovian jump systems under ssynchronous scenario: An optimizing prediction dynamics approach, *IEEE Trans. Autom. Control*, **67** (2022), 4900–4907. https://doi.org/10.1109/TAC.2022.3164832
25. G. Chen, L. Wang, J. Xia, X. Xie, J. H. Park, Data-driven aperiodic sampled-data control of Markovian jump system, *IEEE Trans. Syst. Man Cybern.: Syst.*, **55** (2025), 3338–3349. https://doi.org/10.1109/TSMC.2025.3540568
26. X. Liu, Y. Liang, S. Qiao, P. Wang, Memory-based event-triggered fault-tolerant load frequency control of multi-area power systems with electric vehicles, *Appl. Math. Comput.*, **472** (2024), 128636. https://doi.org/10.1016/j.amc.2024.128636
27. S. Kuppusamy, Y. H. Joo, H. S. Kim, Asynchronous control for discrete-time hidden Markov jump power systems, *IEEE Trans. Cybern.*, **52** (2022), 9943–9948. https://doi.org/10.1109/TCYB.2021.3062672
28. A. Bisoffi, C. De Persis, P. Tesi, Trade-offs in learning controllers from noisy data, *Syst. Control Lett.*, **154** (2021), 104985. https://doi.org/10.1016/j.sysconle.2021.104985
29. C. E. de Souza, Robust stability and stabilization of uncertain discrete-time Markovian jump linear systems, *IEEE Trans. Autom. Control*, **51** (2006), 836–841. https://doi.org/10.1109/TAC.2006.875012
30. X. M. Zhang, Q. L. Han, B. L. Zhang, X. H. Ge, D. W. Zhang, Accumulated-state-error-based event-triggered sampling scheme and its application to H_∞ control of sampled-data systems, *Sci. China Inf. Sci.*, **67** (2024), 162206. https://doi.org/10.1007/s11432-023-4038-3

31. X. M. Zhang, Q. L. Han, X. H. Ge, B. L. Zhang, Accumulative-error-based event-triggered control for discrete-time linear systems: A discrete-time looped functional method, *IEEE/CAA J. Autom. Sin.*, **12** (2025), 683–693. https://doi.org/10.1109/JAS.2024.124476

32. X. Ge, Q. L. Han, X. M. Zhang, D. Ding, B. Ning, Distributed coordination control of multi-agent systems under intermittent sampling and communication: A comprehensive survey, *Sci. China Inf. Sci.*, **68** (2025), 151201. https://doi.org/10.1007/s11432-024-4355-1

AIMS Press